Hindawi
Bioinorganic Chemistry and Applications
Volume 2018, Article ID 7029376, 9 pages
https://doi.org/10.1155/2018/7029376

Research Article

The Structures, Spectroscopic Properties, and Photodynamic Reactions of Three $[RuCl(QN)NO]^-$ Complexes (HQN = 8-Hydroxyquinoline and Its Derivatives) as Potential NO-Donating Drugs

Leilei Xie,[1,2] Lifang Liu,[1,2] Wenming Wang,[1,2] Zhiou Ma,[1] Liqun Xu,[1] Xuan Zhao,[3] and Hongfei Wang[1,2]

[1]*Key Laboratory of Chemical Biology and Molecular Engineering of Education Ministry, Institute of Molecular Science, Shanxi University, Taiyuan 030006, China*
[2]*Key Laboratory of Energy Conversion and Storage Materials of Shanxi Province, Institute of Molecular Science, Shanxi University, Taiyuan 030006, China*
[3]*Department of Chemistry, University of Memphis, Memphis, TN 38152, USA*

Correspondence should be addressed to Hongfei Wang; wanghf@sxu.edu.cn

Received 6 December 2017; Revised 21 May 2018; Accepted 2 October 2018; Published 2 December 2018

Academic Editor: Concepción López

The structures and spectral properties of three ruthenium complexes with 8-hydroxyquinoline (Hhqn) and their derivatives 2-methyl-8-quinolinoline (H2mqn) and 2-chloro-8-quiolinoline (H2cqn) as ligands (QN = hqn, 2mqn, or 2cqn) were calculated with density functional theory (DFT) at the B3LYP level. The UV-Vis and IR spectra of the three $[RuCl(QN)NO]^-$ complexes were theoretically assigned via DFT calculations. The calculated spectra reasonably correspond to the experimentally measured spectra. Photoinduced NO release was confirmed through spin trapping of the electron paramagnetic resonance spectroscopy (EPR), and the dynamic process of the NO dissociation upon photoirradiation was monitored using time-resolved infrared (IR) spectroscopy. Moreover, the energy levels and related components of frontier orbitals were further analyzed to understand the electronic effects of the substituent groups at the 2nd position of the ligands on their photochemical reactivity. This study provides the basis for the design of NO donors with potential applications in photodynamic therapy.

1. Introduction

The structure and reactivity of transition-metal-NO complexes have gained significant interest in recent years because of the important role of nitric oxide (NO) as a signaling molecule in biological systems [1–5]. NO plays important functions in various physiological processes [6–9]. Moreover, the active centers of several important biological enzymes contain metal ions bound with the NO ligand; therefore, studies of the structures and spectra of metal-NO complexes are important to understand the dynamic reactivity and their functions.

The utility of ruthenium (Ru) complexes to design potential anticancer drugs and cellular imaging agents has been extensively investigated [10–15]. Compared to iron-based nitrosyl complexes, Ru nitrosyls are promising candidates as potential NO-donating agents for targeted delivery of NO to physiological targets due to their inherent stability and modest photosensitivity [16–21]. Detailed structural and spectroscopic analyses of Ru complexes with different ligands are essential to investigate the kinetic process of the photoreaction. These studies provide a foundation to control NO release at the physiological target.

A series of nitrosylruthenium (Ru-NO) complexes with polypyridyl complexes have been reported. They are coordinated with (N,N) bidentate ligands forming cationing complexes. The cytotoxicity against tumor cell and their vasodilation effects have been studied [20–25]. Here, three

$[RuCl_3(QN)(NO)]^-$ anionic complexes were synthesized using 8-hydroxyquinoline and its derivatives (HQN) as ligands. These ligands are bidentate chelators that bind metal ions via O-N atoms. Figure 1 shows the structures of the $[RuCl_3(QN)(NO)]^-$ complexes and HQN ligands (HQN = 8-hydroxyquinoline (Hhqn), 2-methyl-8-quinolinol (H2mqn), and 2-chloro-8-quinolinol (H2cqn)). DFT calculations allowed the assignment of bands observed in the electronic and IR spectra of the complexes. Furthermore, the behavior of the three complexes upon photoirradiation was investigated using time-resolved spectroscopy technology. The electronic structures and molecular orbitals of these complexes were calculated to better understand the electronic effect of the substituted group at the 2nd position of the ligands. This study provides insight into the photodynamic properties and potential applications of the nitrosylruthenium (II) complexes.

2. Experimental

2.1. Synthesis. Chemical reagents and solvents were purchased from Sigma (St. Louis, MO, USA) and local vendors. The complexes were synthesized according to a previously described method with modifications [26, 27] and characterized by ^{1}H NMR spectroscopy using a Bruker 600 MHz spectrometer.

2.2. Spectra Measurements. After the complexes were dissolved in DMSO, the UV-visible spectra were recorded on a Thermo 220 spectrophotometer. The IR spectra were measured on an IS50R FT-IR spectrometer (Thermo Fisher) from 2000 to 1400 cm^{-1} at 1 cm^{-1} resolution. The sample solutions were added to an IR cell composed of two CaF_2 windows (25 mm in diameter and 2 mm thick), which were separated by an O-shaped 50 μm thick Teflon spacer.

The photoreaction kinetics was monitored via the IR spectra as a function of irradiation time. The IR spectra were recorded simultaneously for 30 min in the CaF_2 windows while being irradiated with a fiber connected to an Xe lamp with 420 nm band-pass filter (0.2 W/cm^2).

The electron paramagnetic resonance (EPR) spectra were obtained using a Bruker ESP-500E spectrometer at 9.8 GHz, X band, with 100 Hz field modulation. The three complexes (5 mM) mixed with 5 mM $Fe(MGD)_2$ were quantitatively injected into quartz capillaries, respectively. The sample was then illuminated in the cavity of the EPR spectrometer with an Hg lamp (LOT-QuantumDesign GmbH) at 365 nm. All experiments were performed at room temperature (20°C).

2.3. Quantum Chemical Calculations. Gaussian 09 and Gaussview 5 program packages were used for calculations and structure visualization, respectively [28, 29]. The original models for the three complexes were built based on the crystal structure of $[(CH_3)_4N][RuCl(2cqn)NO]$ complex [27]. All structures were fully optimized with Becke's three-parameter hybrid functional and the Lee–Yang–Parr correlation functional (B3LYP) [30–32] in the DMSO solvent. The basis sets aug-cc-pVDZ-PP and 6-311++G(d,p) were used to describe the Ru atom and the ligand atoms, respectively [33, 34]. The charge was set to −1, and both S = 0 and S = 1 states for the complexes were optimized.

The UV-visible spectra for the three complexes in DMSO solution were simulated with a time-dependent (TD-DFT) method, respectively, and the solvent effect was considered via the polarization continuum model [35, 36]. The natural atomic charges and Wiberg bond index of the complexes were obtained by natural population analysis (NPA) and natural bond orbital (NBO) analysis [37, 38].

3. Results and Discussion

3.1. Molecular Geometry. The selected and calculated bond lengths and the angles for three complexes are listed in Table 1. Most of the calculated bond lengths and angles of the optimized geometries (Table 1) deviate from crystal structural data by 0.03 Å and 2°, respectively. The theoretical bond lengths of Ru-N2, Ru-O1, and N2-O2 in $[RuCl_3(2cqn)NO]^-$ complex deviate the experimental data less than 0.01 Å, which is near to the uncertainty caused by the experiment measurements [39, 40].

The structures for both S = 0 and S = 1 as potential ground states were optimized, respectively. As shown in Table 2, the angles of the Ru-NO in the optimized structures of the lowest triplet excited states for three complexes are 143.2, 177.1, and 177.4 degrees, respectively. It is worth noting that the Ru-NO is in the bending model for $[RuCl_3(hqn)NO]^-$ in the triplet excited states. However, they are linear for both $[RuCl_3(2mqn)NO]^-$ and $[RuCl_3(2cqn)NO]^-$ in the singlet state and the lowest-triplet excited states. The calculated energy of the singlet state is the lowest one, suggesting the complexes with diamagnetic ground states.

3.2. Molecular Orbital Analyses. The HOMO-LUMO interactions were calculated to probe the reactivity of the various molecular systems [41–45]. The contour plots of the frontier orbitals for three complexes are shown in Figure 2, and the calculated HOMO and LUMO energy levels are shown in Table 2. The calculations were performed with the DMSO solvent. In the three complexes, the HOMO is described as a QN ligand-based orbital that contains some Ru (d) and NO (p) character, while the LUMO contains an antibonding overlap of the Ru (d) and π^* NO (p) orbitals. It suggests that the (Ru(II)-NO^+) group plays an important role in the photochemical reaction of nitrosylruthenium (II) complexes containing 8-quinoliolate and its derivatives.

For the $[RuCl_3(2mqn)NO]^-$ complex, the HOMO and LUMO relative orbital energies are higher and its LUMO-HOMO gap is smaller than those of $[RuCl_3(hqn)NO]^-$ complex. However, the HOMO and LUMO relative orbital energy is lower for $[RuCl_3(2cqn)NO]^-$ complex, while its LUMO-HOMO gap is larger than $[RuCl_3(hqn)NO]^-$. The variation of HOMO and LUMO energy orbitals suggests that different substituted groups in the 2nd ligand position could adjust the relative energies of the front orbitals and could affect the stabilities and reactivity of these complexes.

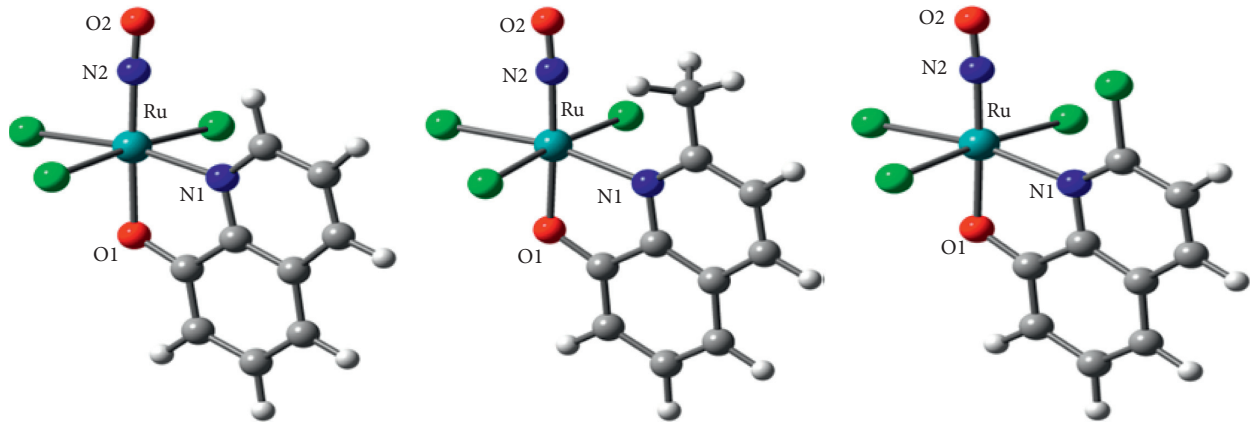

Figure 1: Optimized structures of $[RuCl_3(hqn)NO]^-$ (a), $[RuCl_3(2mqn)NO]^-$ (b), and $[RuCl_3(2cqn)NO]^-$ (c) complexes.

Table 1: Optimized vs. experimental geometries (in Å and °) with 6-311++G(d,p) and Aug-cc-pVDZ-PP as basis set.

	$[RuCl_3(hqn)NO]^-$		$[RuCl_3(2mqn)NO]^-$		$[RuCl_3(2cqn)NO]^-$		X-ray data
	Singlet state	Triplet state	Singlet state	Triplet state	Singlet state	Triplet state	
Ru-N1	2.099	2.087	2.139	2.227	2.154	2.543	2.088
Ru-N2	1.733	1.881	1.734	1.760	1.735	1.758	1.719
Ru-O1	2.011	2.092	1.999	1.981	2.003	1.991	1.993
N2-O2	1.149	1.168	1.148	1.144	1.145	1.144	1.149
∠Ru-N2-O2	177.3	143.2	176.1	177.1	176.0	177.4	174.1

Table 2: Relative energies (kcal/mol) and orbital energies (eV) of HOMOs and LUMOs for $[RuCl_3(hqn)NO]^-$, $[RuCl_3(2mqn)NO]^-$, and $[RuCl_3(2cqn)NO]^-$ complexes.

	$[RuCl_3(hqn)NO]^-$	$[RuCl_3(2mqn)NO]^-$	$[RuCl_3(2cqn)\ NO]^-$
Relative energies ($S = 0$)	−2082.3318613	−2121.6585791	−2541.9469066
Relative energies ($S = 1$)	−2082.291264	−2121.6052187	−2541.8973426
$\Delta_{(S1\text{-}S0)}$	25.475	33.484	31.102
LUMO	−2.728	−2.708	−2.762
LUMO-HOMO gap	3.207	3.164	3.222
HOMO	−5.935	−5.872	−5.984

3.3. Electronic Absorption Spectra. The UV-visible absorption spectra of the three $[RuCl_3(QN)NO]^-$ complexes in DMSO are shown in Figure 3. These three complexes have similar absorption curves in the ultraviolet and visible region with a 11 nm shift in the absorption peak and a 21 nm shift in the absorption peak between $[RuCl_3(2mqn)NO]^-$ and $[RuCl_3(2cqn)NO]^-$ in the ultraviolet region, respectively. In the visible region, the maximum absorption band is at 415 nm for $[RuCl_3(hqn)NO]^-$, 424 nm for $[RuCl_3(2mqn)\ NO]^-$, and 430 nm for $[RuCl_3(2cqn)NO]^-$.

In the UV region, the three complexes display absorption bands at 274 and 337 nm, 270 and 323 nm, 281 and 344 nm, respectively. The corresponding calculated values are 250 and 336 nm, 255 and 331 nm, 262 and 346 nm, respectively. The calculated wavelengths have an error of less than 24 nm compared to the experimental data from the TDDFT method while taking into account of the solvent effect.

The lowest-energy peak near 430 nm predominates the HOMOs-LUMOs excitation in the visible region. The absorption peaks for three complexes were calculated to be near 441, 467, and 461 nm, with deviation from the experimental value by about 30 nm. Analysis of the electronic structures and orbital components of the complexes indicates that these absorption bands mainly originate from the d(Ru)π + p(QN and Cl ligands) ⟶ (d(Ru) + p^*(NO and QN ligands)) charge transfer processes, which were labeled as MLCT and LMCT processes (L stands for NO, Cl, and QN ligands).

3.4. Infrared Spectra. Figure 4 shows the infrared spectra of the three complexes recorded in DMSO. For comparison, the experimentally observed and calculated vibrational frequencies ranging from 2000 to 1400 cm^{-1} are presented in Table 3. The B3LYP functional tends to overestimate the fundamental normal modes of vibration, and thus the calculated frequencies were scaled with appropriate values to harmonize the theoretical and experimental wavenumbers [46]. In this study, the scale factor is about 0.97.

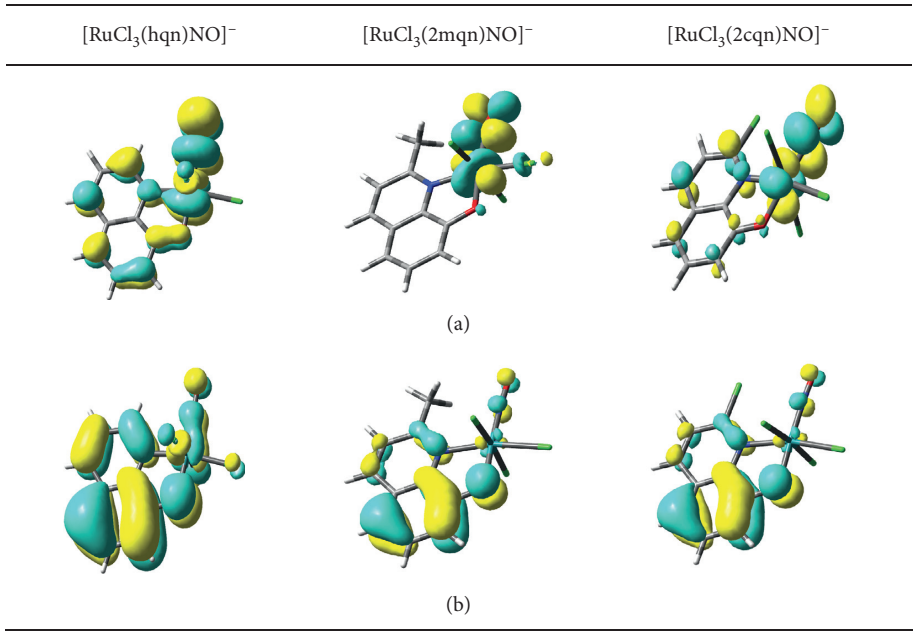

Figure 2: Contour diagrams of the calculated LUMO (a) and HOMO (b) of three complexes. Negative values of the wave function are represented in yellow.

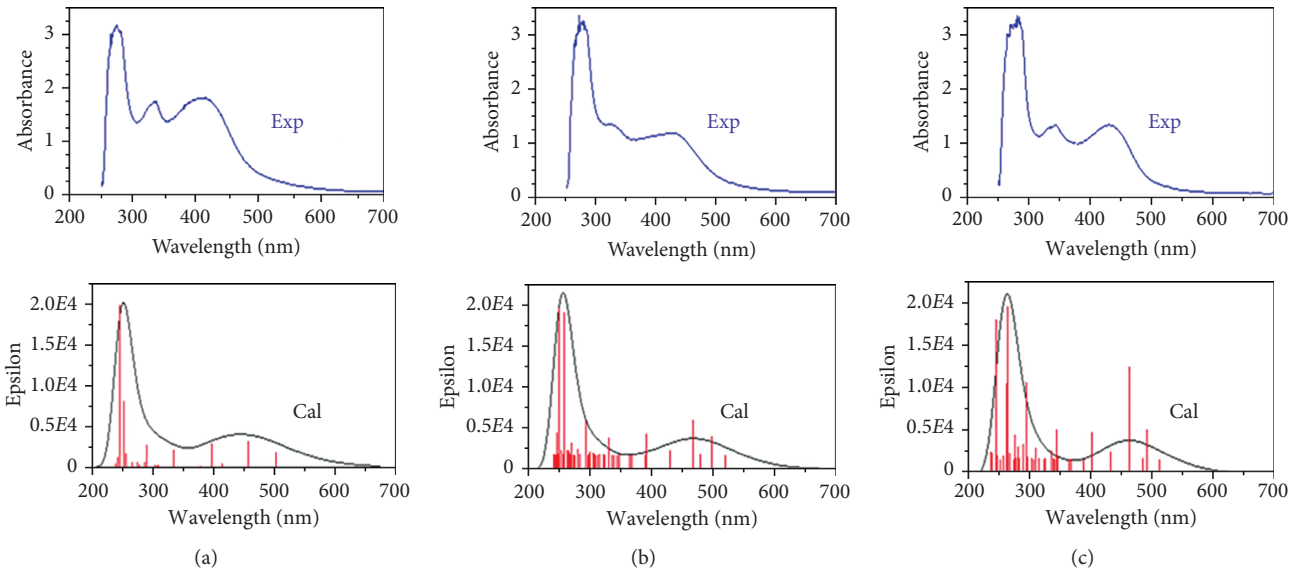

Figure 3: Recorded and calculated electronic absorption spectra of $[RuCl_3(hqn)NO]^-$ (a), $[RuCl_3(2mqn)NO]^-$ (b), and $[RuCl_3(2cqn)NO]^-$ (c) complexes (blue: experimental; black: calculated; red: calculated oscillator strength).

The DFT calculation helps assigning vibrational modes to the observed frequencies. The three important vibrations correspond to the two ligands coordinated to the central Ru. There is a clear and strong vibration peak at ~1840 cm^{-1} that is a stretching vibration for NO in the {Ru(II)-NO^+} group. The vibration peaks at ~1560 and ~1500 cm^{-1} correspond to the vibration of coordinated QN ligands. Monitoring the intensity variation of these peaks offers an important information to investigate the mechanism of the photoinduced reaction of ligand dissociation.

Table 3 lists a comparison of the NO stretching frequencies of the three complexes. Different substituted groups in the 2nd position of the ligand in the [RuCl(2mqn)NO] and [RuCl(hqn)NO] complexes cause a 5 cm^{-1} red shift. This substitution in the [RuCl(2cqn)NO] and [RuCl(hqn)NO] complexes results in a 17 cm^{-1} red shift in the IR absorption peak. Such a shift is clearly a ligand effect; the stretching frequency (ν_{NO}) of three complexes follows this order: ν_{NO} (2cqn) > ν_{NO} (2mqn) > ν_{NO} (hqn). It is clear that ligand substituents could tune the NO stretching frequency in the three nitrosylruthenium complexes.

3.5. Real-Time Measurement of NO Release. The photoinduced NO release from the three complexes was confirmed

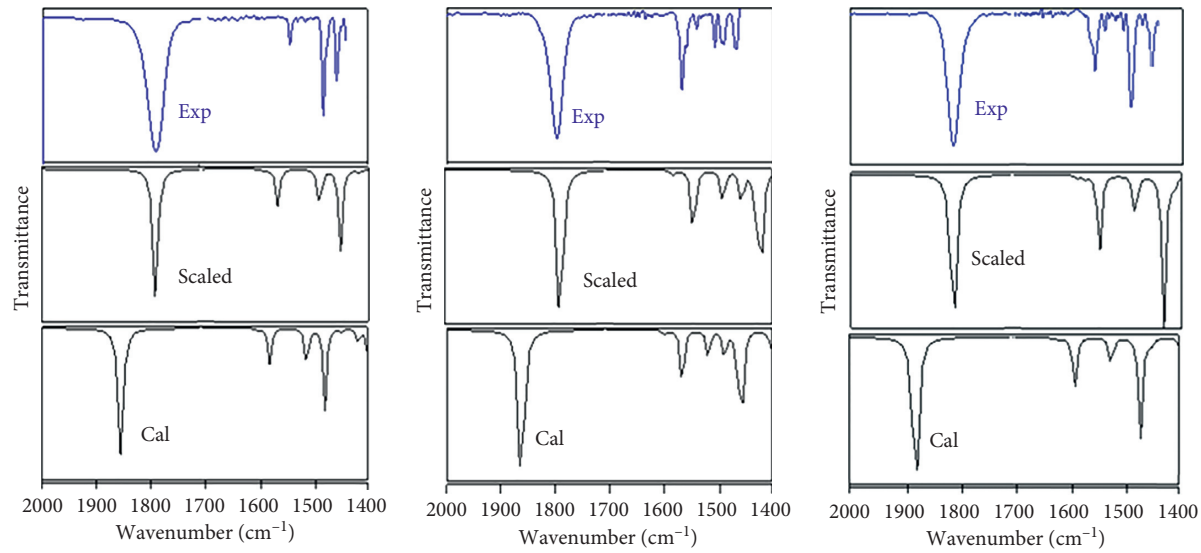

Figure 4: Recorded and calculated IR spectra of $[RuCl_3(hqn)NO]^-$ (a), $[RuCl_3(2mqn)NO]^-$ (b), and $[RuCl_3(2cqn)NO]^-$ (c) complexes in the 2000–1400 cm^{-1} region (blue: experimental; black: calculated).

Table 3: Observed and calculated vibrational frequencies (cm^{-1}) and intensities over 2000–1400 cm^{-1} region for $[RuCl_3(hqn)NO]^-$, $[RuCl_3(2mqn)NO]^-$, and $[RuCl_3(2cqn)NO]^-$ complexes.

$[RuCl_3(hqn)NO]^-$		$[RuCl_3(2mqn)NO]^-$		$[RuCl_3(2cqn)NO]^-$		Assignment
Exp.	Cal.	Exp.	Cal.	Exp.	Cal.	
1839.40	1889.44	1844.01	1894.38	1856.55	1906.72	$\nu_{N=O}$: vs
1576.49	1609.36					δ_{hqn} : m
1500.01	1530.48					δ_{hqn} : m
1470.07	1491.36					δ_{hqn} : m
		1567.78	1593.19			δ_{2mqn} : m
		1540.36	1537.52			δ_{2mqn} : m
		1507.06	1502.23			δ_{2mqn} : m
		1468.27	1472.73			δ_{2mqn} : m
				1558.68	1590.61	δ_{2cqn} : m
				1493.57	1523.66	δ_{2cqn} : m
				1450.55	1470.57	δ_{2cqn} : m

with spin-trapping EPR spectroscopy via $Fe(MGD)_2$ for detecting NO· in real-time [47, 48]. Figure 5 shows the characteristic triplet signal with a hyperfine splitting constant (hfsc) value of 12.78 G and a g-factor of 2.039. These are consistent with published values for NO-Fe^{2+}-MGD adducts [49, 50]. It is obvious that free radicals were generated from the complexes with 365 nm photoirradiation, while almost no signal was observed in the dark. The intensity of resulting free radicals increased quickly upon photoirradiation, reaching a maximum at 30 seconds (Figure 5). It then decreased slowly over 5 minutes. Therefore, the NO release could be controlled with photoirradiation, providing the basis for further applications in photobiology and medicine.

3.6. NBO Analysis. The natural atomic charges of the three complexes were obtained via natural population analysis (NPA) using the B3LYP method (Table 4). In the {Ru-NO} groups, all N atoms have a net positive charge from 0.451 to 0.467. The electronegative oxygen atoms have negative charges from −0.189 to −0.210, respectively. The calculated Wiberg bond index of NO increases from 1.8449 to 1.8501 and 1.8757 in the order of hqn, 2mqn, and 2cqn complexes. The NO stretching frequency (ν_{NO}) shifts from 1839.4 to 1844.01 and 1856.5 cm^{-1}, which is in agreement with the bond order analyses. The Wiberg bond index of Ru-N decreases from 1.6503 to 1.6408 and 1.6251 for the hqn, 2mqn, and 2cqn complexes, respectively, suggesting that NO is relatively easily released from the 2cqn complex. The results agree with the IR spectral measurements below.

3.7. Photoinduced NO Release. Next, photoinduced NO release from the three $[RuCl_3(QN)(NO)]^-$ complexes was investigated using time-resolved IR spectra. A series of FT-IR spectra of the NO stretching mode were recorded as a function of photoirradiation. Figure 6 shows the change in the spectra over time. There is a significant decrease in the intensity of the NO vibrational peak around 1850 cm^{-1}, which dominated the photoinduced NO dissociation. The electronic transition from the metal and QN/Cl ligands to the antibonding orbitals of the $\{Ru(II)\text{-}NO^+\}$ group upon photoirradiation weakens the bonding of Ru-NO and leads to dissociation of NO [51–53]. In addition, the decrease in the NO vibrational intensity for $[RuCl(2cqn)NO]^-$ complex is fast relative to the other two complexes, and its half-life of NO dissociation is shorter. Therefore, NO release could be adjusted by complexes using different ligands upon photoirradiation. This strategy can be applied for NO-donor design with potential applications in photobiology and clinical therapy.

Recently, we studied the cytotoxicity and photo-enhanced cytotoxicity of the three $[Ru(II)Cl_3(QN)(NO)]^-$

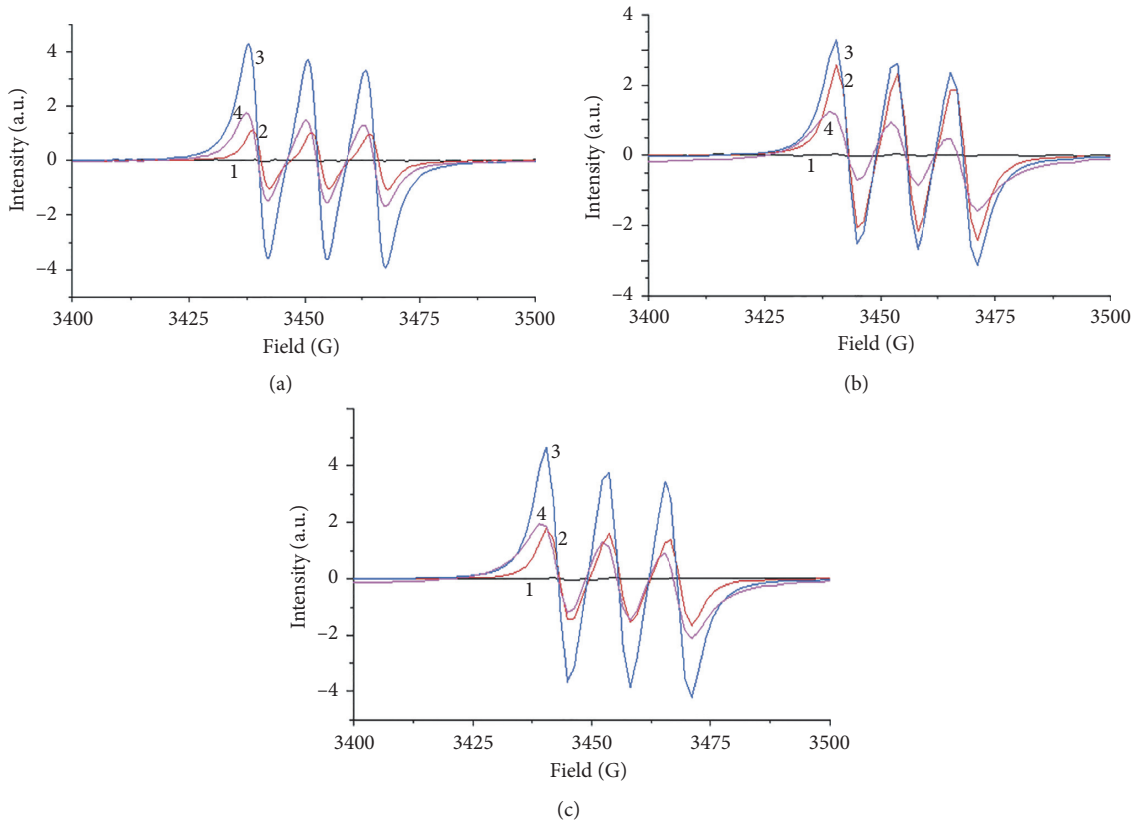

Figure 5: EPR spectra of $[RuCl_3(hqn)NO]^-$ (a), $[RuCl_3(2mqn)NO]^-$ (b), and $[RuCl_3(2cqn)NO]^-$ (c) complexes (1: control, without photoirradiation; 2: 15 s; 3: 30 s; 4: 5 min).

Table 4: Natural atomic charges and Wiberg bond index of NO in the three $[RuCl(QN)NO]^-$ complexes.

Molecule	Peak position/cm^{-1}(exp)	Atomic charge		Wiberg bond index	
		N	O	Ru-N	N-O
$[RuCl(hqn)NO]^-$	1839.40	0.454	−0.210	1.6503	1.8449
$[RuCl(2mqn)NO]^-$	1844.01	0.451	−0.208	1.6408	1.8501
$[RuCl(2cqn)NO]^-$	1856.55	0.467	−0.189	1.6251	1.8757

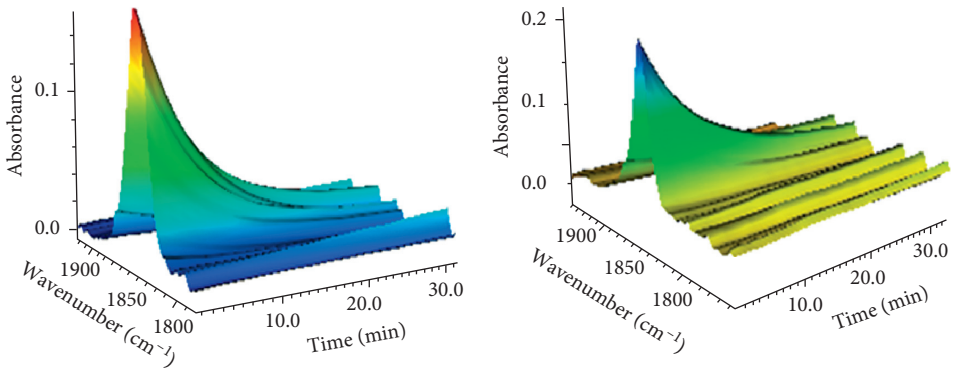

Figure 6: Continued.

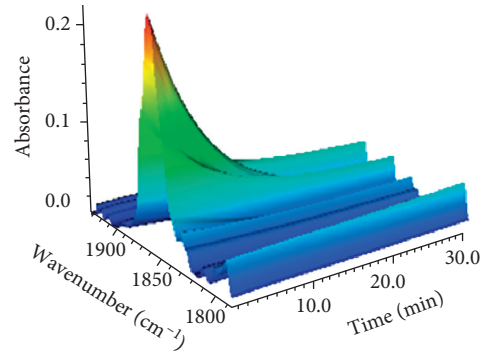

(c)

Figure 6: Time resolution of FT-IR spectra of $[RuCl_3(hqn)NO]^-$ (a), $[RuCl_3(2mqn)NO]^-$ (b), and $[RuCl_3(2cqn)NO]^-$ (c) complexes upon photoirradiation.

complexes against HepG-2 cells [27]. The NO free radicals and $[Ru(III)Cl_3(QN)]^-$ complexes resulting from photoirradiation of these complexes are bioactive and cytotoxic and can serve as the potential drugs with dual functions.

4. Conclusions

We have shown good agreement between the optimized structural parameters and their crystal structures via DFT calculation at the B3LYP level. The results provide valuable geometrical information and help to assign UV-visible spectra and FT-IR spectra. Meanwhile, DFT calculations for electronic structures and spectral characteristics of $[RuCl_3(QN)(NO)]^-$ complexes provide a better understanding of the photophysical and photochemical properties of these complexes. Real-time NO release was studied via spin trapping of the EPR spectroscopy, and the time-resolved IR spectra showed that three complexes have slightly different half-lives of NO dissociation upon photoirradiation. Moreover, an energy level and component analysis of frontier orbitals shows that the different substituent groups at the 2nd position of the ligands affect their reactivities. This study provides the basis for the design of NO donors for their potential applications in photodynamic therapy.

Conflicts of Interest

The authors declare that there are no conflicts of interest.

Acknowledgments

The work was supported partially by the National Natural Science Foundation of China (21671125, 21601112, and 21543003) and by Talent Plan and Research Projects of Shanxi Province (2015081049 and 2015-021). The beam time provided by beamline 3W1A of Beijing Synchrotron Radiation Facility (BSRF) and BL17U and BL18U of the Shanghai Synchrotron Radiation Facility (SSRF) is specially acknowledged.

References

[1] E. G. Abucayon, D. R. Powell, and G. B. Richter-Addo, "Carbon-nitrogen and nitrogen-nitrogen bond formation from nucleophilic attack at coordinated nitrosyls in Fe and Ru Heme models," *Journal of the American Chemical Society*, vol. 139, no. 28, pp. 9495–9498, 2017.

[2] M. A. Herzik, R. Jonnalagadda, J. Kuriyan, and M. A. Marletta, "Structural insights into the role of iron-histidine bond cleavage in nitric oxide-induced activation of H-NOX gas sensor proteins," *Proceedings of the National Academy of Sciences of the United States of America*, vol. 111, no. 40, pp. 4156–4164, 2014.

[3] P. C. Ford, B. O. Fernandez, and M. D. Lim, "Mechanisms of reductive nitrosylation in iron and copper models relevant to biological systems," *Chemical Reviews*, vol. 105, no. 6, pp. 2439–2455, 2005.

[4] F. G. Doro, K. Q. Ferreira, Z. N. da Rocha, G. F. Caramori, A. J. Gomes, and E. Tfouni, "The versatile ruthenium(II/III) tetraazamacrocycle complexes and their nitrosyl derivatives," *Coordination Chemistry Reviews*, vol. 306, no. 2, pp. 652–677, 2016.

[5] M. J. Rose and P. K. Mascharak, "Photoactive ruthenium nitrosyls: effects of light and potential application as NO donors," *Coordination Chemistry Reviews*, vol. 252, no. 18–20, pp. 2093–2114, 2008.

[6] L. J. Ignarro, *Nitric Oxide: Biology and Pathobiology*, Academic Press, Burlington, MA, USA, 2010.

[7] D. Fukumura, S. Kashiwagi, and R. K. Jain, "The role of nitric oxide in tumour progression," *Nature Reviews Cancer*, vol. 6, no. 7, pp. 521–534, 2006.

[8] A. G. Tennyson and S. J. Lippard, "Generation, translocation, and action of nitric oxide in living systems," *Chemistry and Biology*, vol. 18, no. 10, pp. 1211–1220, 2011.

[9] P. T. Burks, J. V. Garcia, R. GonzalezIrias et al., "Nitric oxide releasing materials triggered by near-infrared excitation through tissue filters," *Journal of the American Chemical Society*, vol. 135, no. 48, pp. 18145–18152, 2013.

[10] M. R. Gill and J. A. Thomas, "Ruthenium(II) polypyridyl complexes and DNA—from structural probes to cellular imaging and therapeutics," *Chemical Society Reviews*, vol. 41, no. 8, pp. 3179–3192, 2012.

[11] H. Niyazi, J. P. Hall, K. O'Sullivan et al., "Crystal structures of Λ-$[Ru(phen)_2dppz]^{2+}$with oligonucleotides containing TA/

TA and AT/AT steps show two intercalation modes," *Nature Chemistry*, vol. 4, no. 8, pp. 612–628, 2012.

[12] M. A. Sgambellone, A. David, R. N. Garner, K. R. Dunbar, and C. Turro, "Cellular toxicity induced by the photorelease of a caged bioactive molecule: design of a potential dual-action Ru(II) complex," *Journal of the American Chemical Society*, vol. 135, no. 30, pp. 11274–11282, 2013.

[13] L. X. Xue, T. T. Meng, W. Yang, and K. Z. Wang, "Recent advances in ruthenium complex-based light-driven water oxidation catalysts," *Journal of Photochemistry and Photobiology B: Biology*, vol. 152, pp. 95–105, 2015.

[14] N. Deepika, C. S. Devi, Y. P. Kumar et al., "DNA-binding, cytotoxicity, cellular uptake, apoptosis and photocleavage studies of Ru(II) complexes," *Journal of Photochemistry and Photobiology B-biology*, vol. 160, pp. 142–153, 2016.

[15] M. Schulze, V. Kunz, P. D. Frischmann, and F. Würthner, "A supramolecular ruthenium macrocycle with high catalytic activity for water oxidation that mechanistically mimics photosystem II," *Nature Chemistry*, vol. 8, no. 6, pp. 576–583, 2016.

[16] S. Sen, B. Kawahara, N. L. Fry et al., "A light-activated NO donor attenuates anchorage independent growth of cancer cells: important role of a cross talk between NO and other reactive oxygen species," *Archives of Biochemistry and Biophysics*, vol. 540, no. 1-2, pp. 33–40, 2013.

[17] A. P. de Lima Batista, A. G. S. de Oliveira-Filho, and S. E. Galembeck, "Photophysical properties and the NO photorelease mechanism of a ruthenium nitrosyl model complex investigated using the CASSCF-in-DFT embedding approach," *Physical Chemistry Chemical Physics*, vol. 19, no. 21, pp. 13860–13867, 2017.

[18] H. J. Xiang, Q. Deng, L. An, M. Guo, S. P. Yang, and J. G. Liu, "Tumor cell specific and lysosome-targeted delivery of nitric oxide for enhanced photodynamic therapy triggered by 808 nm near-infrared light," *Chemical Communications*, vol. 52, no. 1, pp. 148–151, 2016.

[19] A. Rathgeb, A. Böhm, M. S. Novak et al., "Ruthenium-nitrosyl complexes with glycine, L-alanine, L-valine, L-proline, D-proline, L-serine, L-threonine, and L-tyrosine: synthesis, X-ray diffraction structures, spectroscopic and electrochemical properties, and antiproliferative activity," *Inorganic Chemistry*, vol. 53, no. 5, pp. 2718–2729, 2014.

[20] M. G. de Oliveira, F. G. Doro, E. Tfouni, and M. H. Krieger, "Phenotypic switching prevention and proliferation/migration inhibition of vascular smooth muscle cells by the ruthenium nitrosyl complex trans-[Ru(NO)Cl(cyclam)](PF6)2," *Journal of Pharmacy and Pharmacology*, vol. 69, no. 9, pp. 1155–1165, 2017.

[21] A. J. Gomes, E. M. Espreafico, and E. Tfouni, "Trans-[Ru(NO)Cl(cyclam)](PF6)2 and [Ru(NO)(Hedta)] incorporated in PLGA nanoparticles for the delivery of nitric oxide to B16-F10 cells: cytotoxicity and phototoxicity," *Molecular Pharmacology*, vol. 10, no. 10, pp. 3544–3554, 2013.

[22] F. P. Rodrigues, C. R. Pestana, A. C. Polizello et al., "Release of NO from a nitrosyl ruthenium complex through oxidation of mitochondrial NADH and effects on mitochondria," *Nitric Oxide-Biology and Chemistry*, vol. 26, no. 3, pp. 174–181, 2012.

[23] A. C. Merkle, A. B. McQuarters, and N. Lehnert, "Synthesis, spectroscopic analysis and photolabilization of water-soluble ruthenium(III)-nitrosyl complexes," *Dalton Transactions*, vol. 41, no. 26, pp. 8047–8059, 2012.

[24] G. J. Rodrigues, A. C. Pereira, T. F. de Moraes, C. C. Wang, R. S. da Silva, and L. M. Bendhack, "Pharmacological characterization of the vasodilating effect induced by the ruthenium complex cis-[Ru(NO)(NO2)(bpy)2](PF6)2," *Journal of Cardiovascular Pharmacology*, vol. 65, no. 2, pp. 168–175, 2015.

[25] P. F. Castro, D. L. de Andrade, F. Reis Cde et al., "Relaxing effect of a new ruthenium complex nitric oxide donor on airway smooth muscle of an experimental model of asthma in rats," *Clinical and Experimental Pharmacology and Physiology*, vol. 43, no. 2, pp. 221–229, 2016.

[26] H. F. Wang, T. Hagihara, H. Ikezawa, H. Tomizawa, and E. Miki, "Electronic effects of the substituent group in 8-quinolinolatoligand on geometrical isomerism for nitrosylruthenium(II)complexes," *Inorganica Chimica Acta*, vol. 299, no. 1, pp. 80–90, 2000.

[27] L. Q. Xu, Z. O. Ma, W. M. Wang et al., "Photo-induced cytotoxicity, photo-controlled nitric oxide release, and DNA/human serum albumin binding of three water-soluble nitrosylruthenium complexes," *Polyhedron*, vol. 137, pp. 157–164, 2017.

[28] M. J. Frisch, G. W. Trucks, H. B. Schlegel et al., *Gaussian 09, revision C.01*, Gaussian, Inc, Wallingford, CT, USA, 2009.

[29] R. Dennington, T. Keith, and J. Millam, *GaussView Version 5*, Semichem Inc., Shawnee Mission KS, 2009.

[30] C. Lee, W. Yang, and R. G. Parr, "Development of the Colle-Salvetti correlation-energy formula into a functional of the electron density," *Physical Review B: Condensed Matter Matter Physics*, vol. 37, no. 2, pp. 785–789, 1988.

[31] A. D. Becke, "Density-functional exchange-energy approximation with correct asymptotic behavior," *Physical Review A General Physics*, vol. 38, no. 6, pp. 3098–3100, 1988.

[32] A. D. Becke, "Density-functional thermochemistry. III. The role of exact exchange," *Journal of Chemical Physics*, vol. 98, no. 7, pp. 5648–5652, 1993.

[33] K. A. Peterson, D. Figgen, M. Dolg, and H. Stoll, "Energy-consistent relativistic pseudopotentials and correlation consistent basis sets for the 4d elements Y-Pd," *Journal of Chemical Physics*, vol. 126, no. 12, pp. 124101–124112, 2007.

[34] W. J. Hehre, L. Radom, P. V. R. Schleyer, and J. Pople, *Ab Initio Molecular Orbital Theory*, Wiley and Sons, New York, NY, USA, 1986.

[35] S. Bhattacharya, T. K. Pradhan, A. De, S. R. Chaudhury, A. K. De, and T. Ganguly, "Photophysical processes involved within the anisole-thioindoxyl dyad system," *Journal of Physical Chemistry A*, vol. 110, no. 17, pp. 5665–5673, 2006.

[36] E. Cances, B. Mennucci, and J. Tomasi, "A new integral equation formalism for the polarizable continuum model: theoretical background and applications to isotropic and anisotropic dielectrics," *Journal of Chemical Physics*, vol. 107, no. 8, pp. 3032–3041, 1997.

[37] R. S. Mulliken, "Electronic population analysis on LCAO-MO molecular wave functions," *Journal of Chemical Physics*, vol. 23, no. 10, pp. 1833–1840, 1955.

[38] E. D. Glendening, A. E. Reed, J. E. Carpenter, and F. Weinhold, *NBO 3.0 Program Manual*, Theoretical Chemistry Institute, University of Wisconsin, Madison, WI, USA, 1990.

[39] R. Akesson, L. G. M. Pettersson, M. Sandstrom, and U. Wahlgren, "Ligand-field effects inthe hydrated divalent and trivalent metal-ions ofthefirst and 2nd transition periods," *Journal of the American Chemical Society*, vol. 116, no. 19, pp. 8691–8704, 1994.

[40] G. Frenking and U. J. Pidu, "Ab initio studies of transition-metal compounds: the nature of the chemical bond to a transition metal," *Journal of the Chemical Society, Dalton Transactions*, no. 10, pp. 1653–1662, 1997.

[41] M. K. Nazeeruddin, F. De Angelis, S. Fantacci et al., "Combined experimental and DFT-TDDFT computational study of photoelectrochemical cell ruthenium sensitizers," *Journal of the American Chemical Society*, vol. 127, no. 48, pp. 16835–16847, 2005.

[42] W. Grochala, A. Albrecht, C. Andreas, and R. Hoffmann, "Remarkably simple relationship connecting the calculated geometries of isomolecular states of three different multiplicities," *Journal of Physical Chemistry*, vol. 104, no. 11, pp. 2195–2203, 2000.

[43] L. Padmaja, M. Amalanathan, C. Ravikumar, and I. Hubert Joe, "NBO analysis and vibrational spectra of 2,6-bis(p-methyl benzylidene cyclohexanone) using density functional theory," *Spectrochimica Acta Part A*, vol. 74, no. 2, pp. 349–356, 2009.

[44] T. S. Sundar, R. Sen, and P. Johari, "Rationally designed donor-acceptor scheme based molecules for applications in opto-electronic devices," *Physical Chemistry Chemical Physics*, vol. 18, no. 13, pp. 9133–9147, 2016.

[45] H. F. Pan, W. M. Wang, Z. O. Ma et al., "Structures and spectroscopic properties of three $[RuCl(2mqn)_2NO]$ (H2mqn = 2-methyl-8-quinolinol) isomers: an experimental and density functional theoretical study," *Polyhedron*, vol. 118, pp. 61–69, 2016.

[46] M. A. Palafox, M. Gill, N. J. Nunez, V. K. Rostogi, L. Mittal, and R. Sharm, "Scaling factors for the prediction of vibrational spectra. II. The aniline molecule and several derivatives," *International Journal of Quantum Chemistry*, vol. 103, no. 4, pp. 394–421, 2005.

[47] A. F. Vanin, A. P. Poltorakov, V. D. Mikoyan, L. N. Kubrina, and E. van Faassen, "Why iron-dithiocarbamates ensure detection of nitric oxide in cells and tissues," *Nitric Oxide*, vol. 15, no. 4, pp. 295–311, 2006.

[48] S. Porasuphatana, J. Weaver, T. A. Budzichowski, P. Tsai, and G. M. Rosen, "Differential effect of buffer on the spin trapping of nitric oxide by iron chelates," *Analytical Biochemistry*, vol. 298, no. 1, pp. 50–56, 2001.

[49] B. Gopalakrishnan, K. M. Nash, M. Velayutham, and F. A. Villamena, "Detection of nitric oxide and superoxide radical anion by electron paramagnetic resonance spectroscopy from cells using spin traps," *Journal of Visualized Experiments*, vol. 66, p. 2810, 2012.

[50] S. Pou, P. Tsai, S. Porasuphatana et al., "Spin trapping of nitric oxide by ferro-chelates: kinetic and in vivo pharmacokinetic studies," *Biochimica ET Biophysica Acta*, vol. 1427, no. 2, pp. 216–226, 1999.

[51] N. L. Fry and P. K. Mascharak, "Photolability of NO in designed metal nitrosyls with carboxamido-N donors: a theoretical attempt to unravel the mechanism," *Dalton Transactions*, vol. 41, no. 16, pp. 4726–4735, 2012.

[52] J. Wang, F. Yang, Y. Zhao et al., "Photoisomerization and structural dynamics of two nitrosylruthenium complexes: a joint study by NMR and nonlinear IR spectroscopies," *Physical Chemistry Chemical Physics*, vol. 16, no. 43, pp. 24045–24054, 2014.

[53] L. Freitag and L. González, "Theoretical spectroscopy and photodynamics of a ruthenium nitrosyl complex," *Inorganic Chemistry*, vol. 53, no. 13, pp. 6415–6426, 2014.